The $C_iC_s(Si_I)_n$ Defect in Silicon from a Density Functional Theory Perspective

Stavros-Richard G. Christopoulos [1], Efstratia N. Sgourou [2], Ruslan V. Vovk [3], Alexander Chroneos [1,4,*] and Charalampos A. Londos [2]

[1] Faculty of Engineering, Environment and Computing, Coventry University, Priory Street, Coventry CV1 5FB, UK; ac0966@coventry.ac.uk

[2] Departmant of Physics, Section of Solid State Physics, National and Kapodistrian University of Athens, Panepistimiopolis Zografos, 157 84 Athens, Greece; e_sgourou@hotmail.com (E.N.S.); hlontos@phys.uoa.gr (C.A.L.)

[3] V. N. Karazin Kharkiv National University, 4 Svobody sq., 61077 Kharkiv, Ukraine; rvvovk2017@gmail.com

[4] Department of Materials, Imperial College London, London SW7 2AZ, UK

[*] Correspondence: alexander.chroneos@imperial.ac.uk; Tel.: +30-697-877-5320

check for updates

Abstract: Carbon constitutes a significant defect in silicon (Si) as it can interact with intrinsic point defects and affect the operation of devices. In heavily irradiated Si containing carbon the initially produced carbon interstitial–carbon substitutional (C_iC_s) defect can associate with self-interstitials (Si_I's) to form, in the course of irradiation, the $C_iC_s(Si_I)$ defect and further form larger complexes namely, $C_iC_s(Si_I)_n$ defects, by the sequential trapping of self-interstitials defects. In the present study, we use density functional theory to clarify the structure and energetics of the $C_iC_s(Si_I)_n$ defects. We report that the lowest energy $C_iC_s(Si_I)$ and $C_iC_s(Si_I)_2$ defects are strongly bound with -2.77 and -5.30 eV, respectively.

1. Introduction

For more than six decades, the rapid evolution of microelectronics has constituted Si as a prevalent material. In the past few years, however, the aim has been to replace Si with other substrates (such as germanium) in nanoelectronic applications. Nevertheless, Si will remain the mainstream material for sensors and photovoltaics [1–10]. From a fundamental solid-state physics perspective, the study of point defects and defect clusters in Si remains of interest, as these can impact its materials properties. This is also technologically motivated, as in order to optimise devices, it is necessary to control the oxygen-related defects (vacancy-oxygen interstitial pairs, VO) as well as the carbon-related defects (such as $C_iC_s(Si_I)_n$ and $C_iO_i(Si_I)_n$, n = 1, 2, . . .) [11–25].

It is established that carbon in Si has a strong tendency to associate with self-interstitials (Si_I's). Indeed, carbon-related defects produced by the irradiation, such as C_iO_i, C_iC_s, and C_i, readily trap Si_I's leading to the formation of larger complexes (for example $C_iO_i(Si_I)_n$, $C_iC_s(Si_I)_n$, and $C_i(Si_I)_n$) [12,14]. This is important, as the existence of these defects restrains the formation of larger Si_I clusters, such as the (113) extended defects, which have detrimental effects in microelectronic devices [26]. Additionally, reaction processes involving the formation of $C_iO_i(Si_I)_n$, $C_iC_s(Si_I)_n$, and $C_i(Si_I)_n$ structures are taken into account when radiation damage data are modeled for the fabrication of Si-tolerant radiation detectors [27,28].

The structure of the $C_iC_s(Si_I)_n$ complexes with n = 2, 3, . . . is not established, and the electrical activity of the members of the family is not known. The C_iC_s center has been detected and reported by

many experimental techniques [28]. Regarding the optical activity, at least 11 local vibration modes have been correlated with the different configurations of the defect, which exhibit metastability [28]. However, only two IR bands have been correlated with the $C_iC_s(Si_I)$ complex and another two with the $C_iC_s(Si_I)_2$ complex [16]. Regarding the electrical activity, at least two levels have been correlated with the C_iC_s defect [28]. However, no levels have been associated with the $C_iC_s(Si_I)_n$ complexes, although it is not unreasonable to expect that levels will be introduced in the gap. To the best of our knowledge, there is no experimental or theoretical study proving that Si_I's passivate the C_iC_s defect. Finally, the C_iC_s defect exhibits metastability [28], although this behavior has not been detected for the $C_iC_s(Si_I)$ complex or the higher order member of the family.

In the present study, we have used extensive density functional theory (DFT) calculations to study the structure and energetics of the $C_iC_s(Si_I)_n$ defects (where n = 0, 1, 2). Based on these calculations, we propose the structure of the $C_iC_s(Si_I)_2$ defect.

2. Methodology

2.1. Details of Calculations

The calculations in this study were performed using the plane wave DFT code Cambridge Serial Total Energy Package (CASTEP) [29]. To account for the exchange and correlation interactions, we implemented the corrected density functional of Perdew, Burke, and Ernzerhof (PBE) [30], within the generalized gradient approximation (GGA) and with ultrasoft pseudopotentials [31]. A 250-atomic site supercell ($5 \times 5 \times 5$ supercell with 2 atoms/primitive cell) was employed under constant pressure conditions. The cut-off of the plane wave basis set was 350 eV, and a $2 \times 2 \times 2$ Monkhorst-Pack (MP) [32] k-point grid was used. This methodology has been employed and discussed in recent studies [33–35].

2.2. Definitions of Binding Energies

To distinguish between the different configurations of the $C_iC_s(Si_I)_n$ defect and to decide which one is favourable, the criterion is the minimization of the binding energy. For example, the binding energy to form a $C_iC_s(Si_I)_2$ defect in Si is

$$E_b[C_iC_s(Si_I)_2Si_N)] = E[C_iC_s(Si_I)_2Si_N)] - E[C_iSi_N] - E[C_sSi_{N-1}] - 2E[Si_ISi_N] - 3E[Si_N] \qquad (1)$$

where $E[C_iC_s(Si_I)_2Si_N]$ is the energy of an N lattice site supercell (here N = 250) containing N Si atoms, a C_i, a C_s atom, two Si_I's, and N Si atoms; $E[C_iSi_N]$ is the energy of a supercell containing a C_i and N Si atoms; $E[C_sSi_{N-1}]$ is the energy of a supercell containing one C_s atom and N − 1 Si atoms; $E[Si_ISi_N]$ is the energy of a supercell containing an Si_I and N Si atoms; $E[Si_N]$ is the energy of the N Si atom supercell. A binding energy effectively means that the defect cluster is stable with respect to its constituent point defect components.

3. Results and Discussion

Here we have applied extensive DFT calculations to find the lowest energy structures of the $C_iC_s(Si_I)_n$ defects (n = 1, 2, . . .). In essence, we used a step-by-step approach, first calculating the minimum energy structure of C_iC_s and then adding one and finally two Si_I's. To explore all possible configurations, we considered numerous calculations (more than 3000) by positioning the constituent defects in all possible sites in the supercell.

In the present study, we worked based on the following steps: (a) Knowing the most favourable position for C_i [10], we determined the binding energy and the position of the C_s substitutional defect for the near and the distant positions in Si positions in the crystal. We found two equivalent positions with a binding energy of −0.90 eV (see Figure 1a). (b) The second step was to add an Si interstitial (Si_I) to the crystal with the most favourable C_s defect. We performed, for this reason, 1000 calculations in a

$10 \times 10 \times 10$ grid in a 13.5 Å $\times$ 13.5 Å $\times$ 13.5 Å cube around C_i and C_s defects. The binding energy of the most favourable Si_I is -2.77 eV (see Figure 1b). (c) The next step was to add a second Si interstitial. Following the same procedure, we performed 1000 calculations in a $10 \times 10 \times 10$ grid in a 13.5 Å $\times$ 13.5 Å $\times$ 13.5 Å cube in order to determine the position and the binding energy of the "second in order" Si interstitial (Si_{I2}) (see Figure 1c). For a better investigation, we also performed the same procedure for the second favourable Si_I. Thus, we ended up with two equivalent positions with a binding energy of -5.30 eV (see Figure 1d).
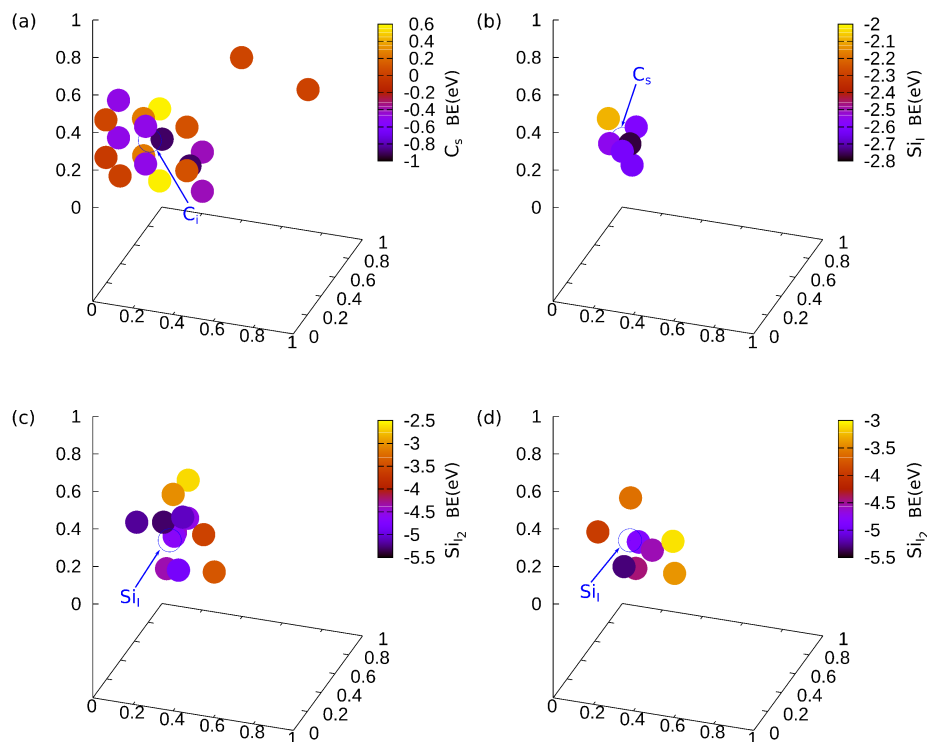

Figure 1. Relative positions of the defects with the lowest binding energy (**a**) of the possible C_s substitutional and the C_i interstitial defect, (**b**) of the "first in order" possible Si interstitial (Si_I) and the chosen C_s substitutional defects, (**c**) of the "second in order" possible Si interstitial (Si_{I2}) and the chosen "first in order" most favourable Si interstitial (Si_I), and (**d**) of the "second in order" possible Si interstitial (Si_{I2}) and the chosen "first in order" second favourable Si interstitial (Si_I). The blue circle denotes the position of the "given" interstitial and the color bar represents the binding energy for each position.

In agreement with previous DFT studies ([36,37] and references therein), the energetically favourable structure of the C_iC_s defect is given in Figure 2a. In this configuration, an Si (marked Si_1 in what follows) at its lattice site separates the C_i and C_s atoms. The angle of $C_iSi_IC_s$ is $121.42°$ (refer to Figure 2a). The binding energy of the C_iC_s defect is calculated to be -0.90 eV, in agreement with previous studies [21,36,37]. Thereafter, we formed the $C_iC_s(Si_I)$ by adding an Si_I to the C_iC_s defect. In this defect, the Si_I atom is 1.88 Å away from the C_i atom (d_3 in Figure 2b), whereas the distances between the carbon defects and the bridging Si atom are significantly extended compared to the C_iC_s defect (compare distances d_1 and d_3 in Figure 2a,b, respectively). Additionally, the presence of the Si_I decreases the angle of $C_iSi_IC_s$ to $118.03°$. This defect is bound with -2.77 eV; i.e., there is an increase in the binding energy by -1.87 eV when an Si_I is associated with the C_iC_s defect (refer to Table 1).
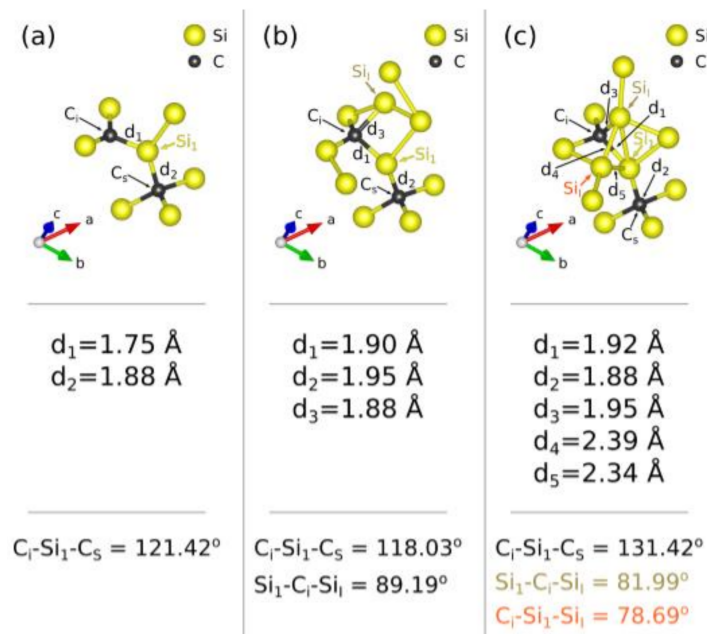
Figure 2. Schematic representation of the energetically favourable (**a**) C_iC_s, (**b**) $C_iC_s(Si_I)$, and (**c**) $C_iC_s(Si_I)_2$ configurations.

Table 1. The binding energies of the $C_iC_s(Si_I)_n$ defects (n = 0, 1, 2) in Si.

Title	BE/eV	BE Difference/eV
C_iC_s	−0.90	-
$C_iC_s(Si_I)$	−2.77	−1.87
$C_iC_s(Si_I)_2$	−5.30	−2.53

The addition of a further Si_I results in the formation of the $C_iC_s(Si_I)_2$ defect (refer to Figure 2c). The binding energy of this defect is −5.30 eV, so there is an increase of the binding energy by −2.53 eV when an Si_I is associated with the $C_iC_s(Si_I)$ defect (refer to Table 1). In this configuration, the first Si_I atom is again in the vicinity of the C_i atom, but the d_3 distance increases to 1.95 Å (refer to Figure 2c). The second Si_I atom is close to the bridging Si_1 atom (d_5 distance being 2.34 Å, Figure 2c). The introduction of the second Si_I atom in the vicinity of the Si_1 atom leads to the extension of the $C_iSi_IC_s$ angle to 131.42°. The distance between the two Si_I atoms is 2.39 Å (d_4 distance, Figure 2c).

Here, the picture is consistent with the experimental viewpoint that the C_iC_s and $C_iC_s(Si_I)$ defects will attract Si_I. In essence, when there is a supersaturation of Si_I, these defects will strongly attract and immobilize the Si_I. The concentration of the $C_iC_s(Si_I)_n$ defects will depend upon the initial carbon concentration of Si and will also require a non-equilibrium concentration of Si_I defects. The latter is because of the high formation energy of Si_I under equilibrium conditions; therefore, $C_iC_s(Si_I)_n$ defects will acquire high concentrations under irradiation or implantation where Si_I's are more abundant. The accumulation of Si_I in the $C_iC_s(Si_I)_n$ defects will impact the properties of Si and the concentration of unbound Si_I.

4. Conclusions

In the present study, DFT calculations were employed to calculate the binding energies and is in essence the structure of the $C_iC_s(Si_I)_n$ defects (n = 0, 1, 2). The structure calculated for C_iC_s is in excellent agreement with previous reports. Here we have calculated the lowest energy structures of the $C_iC_s(Si_I)$ and $C_iC_s(Si_I)_2$ defects by employing a comprehensive technique where all possibilities in a 250-atom supercell are considered. It is calculated that the $C_iC_s(Si_I)$ and $C_iC_s(Si_I)_2$ defects are

strongly bound with −2.77 and −5.30 eV, respectively. This is consistent with experimental work. The electronic structure and energetics of the derived structures should be further investigated using state-of-the-art hybrid functionals. Although the more simple approach used here will yield the right trends, it is anticipated that a hybrid functional will be more appropriate for a detailed understanding of these defects. This study mainly focuses on the binding energies of the $C_iC_s(Si_I)_n$ defects, but it should be stressed that kinetics can play a role in the formation of these defects. Atomistic modelling work in conjunction with thermodynamic models (mass action analysis) [38] is needed to assess the relative importance of the $C_iC_s(Si_I)_n$ defects as compared to competing carbon-related defects such as $C_iO_i(Si_I)_n$.

Author Contributions: Alexander Chroneos and Ruslan V. Vovk conceived and designed the modelling of the system; Stavros-Richard G. Christopoulos performed the calculations; Efstratia N. Sgourou analyzed the data; Alexander Chroneos and Charalampos A. Londos wrote the paper.

Conflicts of Interest: The authors declare no conflict of interest.

References

1. Claeys, C.; Simoen, E. *Germanium-Based Technologies: From Materials to Devices*; Elsevier Science: New York, NY, USA, 2007.
2. Bracht, H.; Chroneos, A. The vacancy in silicon: A critical evaluation of experimental and theoretical studies. *J. Appl. Phys.* **2008**, *104*, 076108. [CrossRef]
3. Chroneos, A.; Grimes, R.W.; Bracht, H. Impact of germanium on vacancy clustering in germanium-doped silicon. *J. Appl. Phys.* **2009**, *105*, 016102. [CrossRef]
4. Wang, H.; Chroneos, A.; Londos, C.A.; Sgourou, E.N.; Schwingenschlögl, U. A-centers in silicon studied with hybrid density functional theory. *Appl. Phys. Lett.* **2013**, *103*, 052101. [CrossRef]
5. Mostafa, A.; Medraj, M. Binary phase diagrams and thermodynamic properties of silicon and essential doping elements (Al, As, B, Bi, Ga, In, N, P, Sb and Tl). *Materials* **2017**, *10*, 676. [CrossRef] [PubMed]
6. Dong, P.; Yu, X.G.; Chen, L.; Ma, X.Y.; Yang, D.R. Effect of germanium doping on the formation kinetics of vacancy-dioxygen complexes in high dose neutron irradiated crystalline silicon. *J. Appl. Phys.* **2017**, *122*, 095704. [CrossRef]
7. Chroneos, A. Effect of carbon on dopant–vacancy pair stability in germanium. *Semicond. Sci. Technol.* **2011**, *26*, 095017. [CrossRef]
8. Sun, J.F.; He, Q.X.; Ban, B.Y.; Bai, X.L.; Li, J.W.; Chen, J. Effect of Sn doping on improvement of minority carrier lifetime of Fe contaminated p-type multi-crystalline Si ingot. *J. Cryst. Growth* **2017**, *458*, 66. [CrossRef]
9. Kube, R.; Bracht, H.; Chroneos, A.; Posselt, M.; Schmidt, B. Intrinsic and extrinsic diffusion of indium in germanium. *J. Appl. Phys.* **2009**, *106*, 063534. [CrossRef]
10. Christopoulos, S.-R.G.; Sgourou, E.N.; Vovk, R.V.; Chroneos, A.; Londos, C.A. Impact of isovalent doping on the formation of the $C_iO_i(Si_I)_n$ defects in silicon. *Solid State Commun.* **2017**, *263*, 19. [CrossRef]
11. Brozel, M.R.; Newman, R.C.; Totterdell, D.H.J. Interstitial defects involving carbon in irradiated silicon. *J. Phys. C Solid State Phys.* **1975**, *8*, 243. [CrossRef]
12. Davies, G.; Lightowlers, E.C.; Newman, R.C.; Oates, A.S. A model for radiation damage effects in carbon-doped crystalline silicon. *Semicond. Sci. Technol.* **1987**, *2*, 524. [CrossRef]
13. Coutinho, J.; Jones, R.; Briddon, P.R.; Öberg, S. Oxygen and dioxygen centers in Si and Ge: Density-functional calculations. *Phys. Rev. B* **2000**, *62*, 10824–10840. [CrossRef]
14. Mattoni, A.; Bernardini, F.; Colombo, L. Self-interstitial trapping by carbon complexes in crystalline silicon. *Phys. Rev. B* **2002**, *66*, 195214. [CrossRef]
15. Londos, C.A.; Potsidi, M.S.; Stakakis, E. Carbon-related complexes in neutron-irradiated silicon. *Phys. B Condens. Matter* **2003**, *340–342*, 551–555. [CrossRef]
16. Potsidi, M.S.; Londos, C.A. The CiCs(SiI) defect in silicon: An infrared spectroscopy study. *J. Appl. Phys.* **2006**, *100*, 033523. [CrossRef]
17. Murin, L.I.; Lindström, J.L.; Davies, G.; Markevich, V.P. Evolution of radiation-induced carbon–oxygen-related defects in silicon upon annealing: LVM studies. *Nucl. Instrum. Methods Phys. Res. Sect. B Beam Interact. Mater. At.* **2006**, *253*, 210–213. [CrossRef]

18. Londos, C.A.; Andrianakis, A.; Emtsev, V.V.; Ohyama, H. Radiation-induced defects in Czochralski-grown silicon containing carbon and germanium. *Semicond. Sci. Technol.* **2009**, *24*, 075002. [CrossRef]

19. Chroneos, A.; Londos, C.A.; Sgourou, E.N.; Pochet, P. Point defect engineering strategies to suppress A-center formation in silicon. *Appl. Phys. Lett.* **2011**, *99*, 241901. [CrossRef]

20. Chroneos, A. Effect of germanium substrate loss and nitrogen on dopant diffusion in germanium. *J. Appl. Phys.* **2009**, *105*, 056101. [CrossRef]

21. Wang, H.; Chroneos, A.; Londos, C.A.; Sgourou, E.N.; Schwingenschlögl, U. Carbon related defects in irradiated silicon revisited. *Sci. Rep.* **2014**, *4*, 4909. [CrossRef] [PubMed]

22. Murin, L.I.; Svensson, B.G.; Markevich, V.P.; Peaker, A.R. Interactions of Self-Interstitials with Interstitial Carbon-Interstitial Oxygen Center in Irradiated Silicon: An Infrared Absorption Study. *Solid State Phenom.* **2014**, *205–206*, 218–223. [CrossRef]

23. Chroneos, A.; Sgourou, E.N.; Londos, C.A.; Schwingenschlögl, U. Oxygen defect processes in silicon and silicon germanium. *Appl. Phys. Rev.* **2015**, *2*, 021306. [CrossRef]

24. Angeletos, T.; Chroneos, A.; Londos, C.A. Infrared studies of the evolution of the CiOi(SiI) defect in irradiated Si upon isothermal anneals. *J. Appl. Phys.* **2016**, *119*, 125704. [CrossRef]

25. Beaufils, C.; Redjem, W.; Rousseau, E.; Jacques, V.; Kuznetsov, A.Y.; Raynaud, C.; Voisin, C.; Benali, A.; Herzig, T.; Pezzagna, S.; et al. Optical properties of an ensemble of G-centers in silicon. *Phys. Rev. B* **2018**, *97*, 035303. [CrossRef]

26. Stiebel, D.; Pichler, P.; Cowern, N.E.B. A reduced approach for modeling the influence of nanoclusters and {113} defects on transient enhanced diffusion. *Appl. Phys. Lett.* **2001**, *79*, 2654–2656. [CrossRef]

27. Huhtinen, M. Simulation of non-ionising energy loss and defect formation in silicon. *Nucl. Instrum. Methods Phys. Res. Sect. Accel. Spectrom. Detect. Assoc. Equip.* **2002**, *491*, 194–215. [CrossRef]

28. Docaj, A.; Estreicher, S.K. Three carbon pairs in Si. In Proceedings of the 26th International Conference on Defects in Semiconductors, Nelson, New Zealand, 17–22 July 2012; Volume 407, pp. 2981–2984. [CrossRef]

29. Payne, M.C.; Teter, M.P.; Allan, D.C.; Arias, T.A.; Joannopoulos, J.D. Iterative minimization techniques for ab initio total-energy calculations: Molecular dynamics and conjugate gradients. *Rev. Mod. Phys.* **1992**, *64*, 1045–1097. [CrossRef]

30. Segall, M.D.; Lindan, P.J.D.; Probert, M.J.; Pickard, C.J.; Hasnip, P.J.; Clark, S.J.; Payne, M.C. First-principles simulation: Ideas, illustrations and the CASTEP code. *J. Phys. Condens. Matter* **2002**, *14*, 2717. [CrossRef]

31. Perdew, J.P.; Burke, K.; Ernzerhof, M. Generalized Gradient Approximation Made Simple. *Phys. Rev. Lett.* **1996**, *77*, 3865–3868. [CrossRef] [PubMed]

32. Vanderbilt, D. Soft self-consistent pseudopotentials in a generalized eigenvalue formalism. *Phys. Rev. B* **1990**, *41*, 7892–7895. [CrossRef]

33. Monkhorst, H.J.; Pack, J.D. Special points for Brillouin-zone integrations. *Phys. Rev. B* **1976**, *13*, 5188–5192. [CrossRef]

34. Chroneos, A.; Londos, C.A. Interaction of A-centers with isovalent impurities in silicon. *J. Appl. Phys.* **2010**, *107*, 093518. [CrossRef]

35. Chroneos, A.; Londos, C.A.; Bracht, H. A-centers and isovalent impurities in germanium: Density functional theory calculations. *Mater. Sci. Eng. B* **2011**, *176*, 453–457. [CrossRef]

36. Zirkelbach, F.; Stritzker, B.; Nordlund, K.; Lindner, J.K.N.; Schmidt, W.G.; Rauls, E. Combined ab initio and classical potential simulation study on silicon carbide precipitation in silicon. *Phys. Rev. B* **2011**, *84*, 064126. [CrossRef]

37. Sgourou, E.N.; Timerkaeva, D.; Londos, C.A.; Aliprantis, D.; Chroneos, A.; Caliste, D.; Pochet, P. Impact of isovalent doping on the trapping of vacancy and interstitial related defects in Si. *J. Appl. Phys.* **2013**, *113*, 239901. [CrossRef]

38. Kröger, F.A.; Vink, H.J. Relations between the Concentrations of Imperfections in Crystalline Solids. In *Solid State Physics*; Seitz, F., Turnbull, D., Eds.; Academic Press: Cambridge, MA, USA, 1956; Volume 3, pp. 307–345, ISBN 0081-1947. [CrossRef]